Continuum-scale simulation tools for transport phenomena in dense suspensions

Pranay P. Nagrani

PIs:

Dr. Ivan C. Christov and Dr. Amy M. Marconnet

in collaboration with Dr. Federico Municchi (Colorado School of Mines)

School of Mechanical Engineering
Purdue University
West Lafayette, Indiana

TMNT-Lab

PURDUE UNIVERSITY | School of Mechanical Engineering

Introduction: Suspensions

Definition

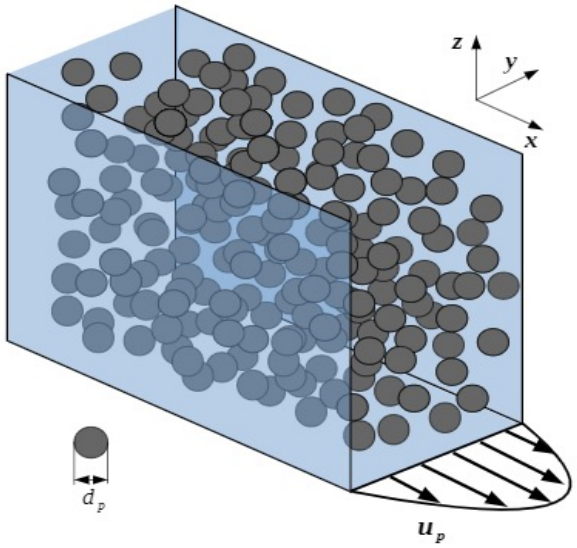

(Dontsov & Peirce, 2015)

- A **suspension** is a dispersion of solid particles ($d_p > 1\ \mu\text{m}$) in a fluid medium (typically Newtonian).
- A **dense** (or 'concentrated') suspension involves a bulk particle volume fraction $\phi > 30\%$.

Particle Migration

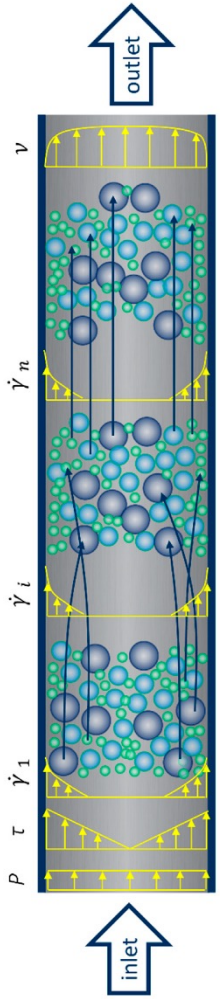

- **Stress inhomogeneity** causes a particles migration flux centerline.

(Gadala-Maria, Leighton, Acrivos, Phillips *et al*, ca. 1987-95)

- This shear-induced migration occurs **from high shear rate to low shear** rate regions.
- Most prominent in **highly viscous** ($Re_{\dot{\gamma}} = \rho_f d_p^2 \dot{\gamma}/\mu_f \ll 1$) and **non-Brownian** ($Pe_{\dot{\gamma}} = d_p^2 \dot{\gamma}/D_T \gg 1$) flows.

(Here, $D_T = 6\pi d_p \mu_f / k_B T$ from Stokes-Einstein)

(figure from Fataei *et al.*, *Materials* 2020)

Applications of dense suspensions

Proppants in hydraulic fracturing

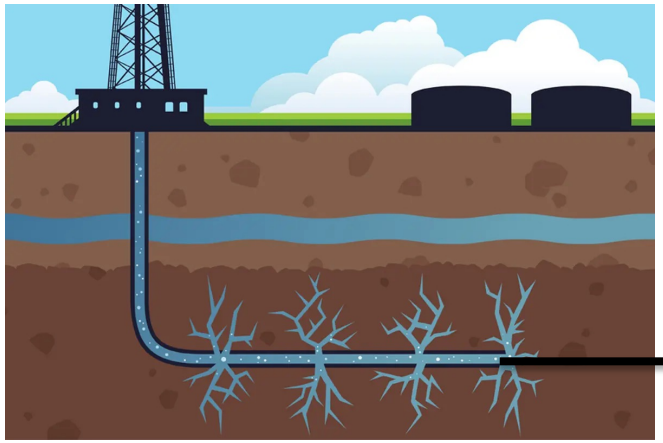

(Figure from: https://www.texastribune.org/2011/07/28/epa-issues-new-standards-hydraulic-fracturing/)

Migration of red blood cells

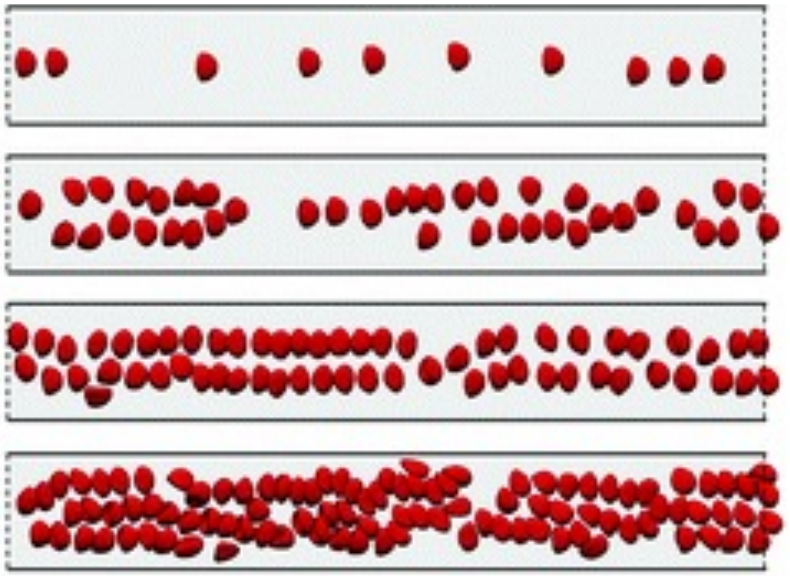

(Iss *et al.*, Soft matter, 2019)

- Inertia and shear-induced migration case RBCs to accumulate near centerline.

Electronics cooling

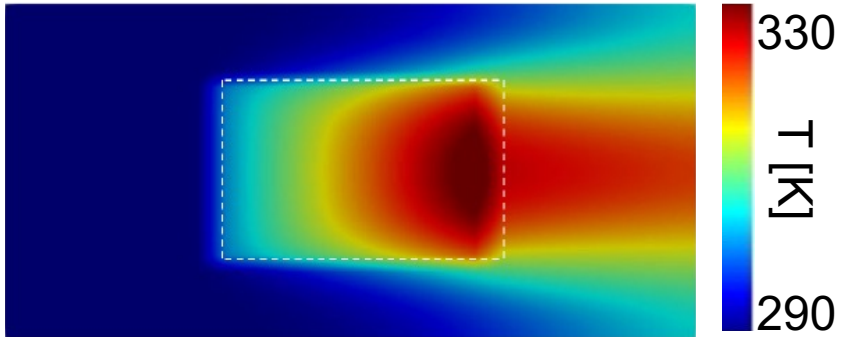

(Nagrani, Christov, and Marconnet, IEEE-ITherm:, 2021)

- Flow of suspension in microchannels mitigate junction level temperature rise.

Two-fluid model (TFM)

- Two different set of equations for particles and fluid each modeled as a continuum:

$$\frac{\partial \phi}{\partial t} + \nabla \cdot (\boldsymbol{u}_p \phi) = 0$$

$$\frac{\partial}{\partial t}(1-\phi) + \nabla \cdot [\boldsymbol{u}_f (1-\phi)] = 0$$

$$\frac{\partial}{\partial t}[\rho_f (1-\phi)\boldsymbol{u}_f] + \nabla \cdot [\rho_f (1-\phi)\boldsymbol{u}_f \boldsymbol{u}_f] = \nabla \cdot \boldsymbol{\Sigma}_f - \boldsymbol{f}_d + (1-\phi)\rho_f \boldsymbol{g}$$

$$\frac{\partial}{\partial t}(\rho_p \phi \boldsymbol{u}_p) + \nabla \cdot (\rho_p \phi \boldsymbol{u}_p \boldsymbol{u}_p) = \nabla \cdot \boldsymbol{\Sigma}_p + \phi \rho_p \boldsymbol{g} + \boldsymbol{f}_d$$

- **Particle and fluid rheology are separated** in the respective stress tensors $\boldsymbol{\Sigma}_p$ and $\boldsymbol{\Sigma}_f$.
  - TFM can reproduce results of the suspension balance model in general curvilinear flows without models to account for rotation – easier to incorporate 'flow-aligned' tensor models.

- Momentum equations are coupled by an interphase drag force $\boldsymbol{f}_d$ (closed using Clift drag).

ρ = density
ϕ = particle volume fraction
t = time
Σ = stress tensor
$\boldsymbol{u}$ = velocity

p: particle
f: fluid

$\boldsymbol{f}_d$ = interphase drag force
g = acceleration due to gravity

Implemented the OpenFOAM® – A Finite Volume Library
Github code: https://github.com/fmuni/twoFluidsNBSuspensionFoam

Validation in Couette cell:

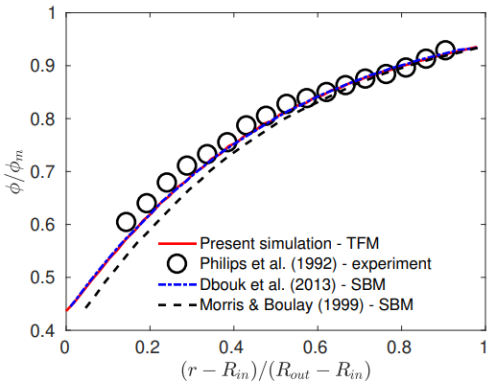

Municchi, Nagrani & Christov, *Int. J. Multiphase Flow*, 2019

Two-fluid modeling: thermal transport

Energy balances in particles and fluid phases:

unsteady | convection | pressure work | conduction | inter-phase heat transfer

$$\frac{\partial}{\partial t}\left(\rho_p \phi H_p\right) + \nabla \cdot \left(\rho_p \phi H_p \boldsymbol{u}_p\right) = \phi \frac{\partial p}{\partial t} + \nabla \cdot \left(\rho_p \alpha_p \phi \nabla e_p\right) - K_h (T_p - T_f)$$

$$\frac{\partial}{\partial t}\left(\rho_f (1-\phi) H_f\right) + \nabla \cdot \left(\rho_f (1-\phi) H_f \boldsymbol{u}_f\right) = (1-\phi) \frac{\partial p}{\partial t} + \nabla \cdot \left(\rho_f \alpha_f (1-\phi) \nabla e_f\right) + K_h (T_p - T_f)$$

K_h: interphase heat transfer coefficient (unknown)

Capturing enhancement of interphase heat transfer:

$$K_h = K_{h_o}\left(1 + \beta\phi\left(\frac{||\dot{\boldsymbol{S}}_{\boldsymbol{p}}|| d_p^2}{\alpha_p}\right)^m\right)$$

proposed closure relation

At zero shear:

$$K_{h_o} = \frac{Nu_{d_p} k_f}{d_p^2}$$

$$Nu_{d_p} = 2 + 0.6 Pr^{0.3} Re^{0.5}$$

(Ranz & Marshall, *Chem. Eng. Prog.*, 1952)

$\dot{\boldsymbol{S}}_p$ = deviatoric rate of particle strain
d_p = particle diameter
α = thermal diffusivity
β, m = fitting parameters

ρ = density
ϕ = particle concentration
H = enthalpy
e = internal Energy
$\boldsymbol{u}$ = velocity
T = temperature
p = pressure

Subscripts:
p: particle
f: fluid

The shear-induced particle stress

- Normal stress differences arise from the stress anisotropy

- Total particle phase stress

$$\boldsymbol{\Sigma}_p = 2\mu_p \dot{\boldsymbol{S}}_p + \boldsymbol{\Sigma}_s$$

where

$$\dot{\boldsymbol{S}}_p = \frac{1}{2}\left[\nabla \boldsymbol{u}_p + \left(\nabla \boldsymbol{u}_p\right)^T\right] - (\nabla \cdot \boldsymbol{u}_p) I$$

- Shear-induced extra stress

$$\boldsymbol{\Sigma}_s = \boldsymbol{\Sigma}_s(\phi, \dot{\gamma}) = -\mu_f \eta_N(\phi) \dot{\gamma}_{\text{eff}} \boldsymbol{Q}(\phi)$$

where

$$\dot{\gamma}_{\text{eff}} = \sqrt{2\dot{\boldsymbol{S}}_p : \dot{\boldsymbol{S}}_p}$$

μ = Dynamic Viscosity

$\dot{\boldsymbol{S}}$ = Deviatoric rate of strain

$\eta_N(\phi)$ = Normal Scaled Viscosity

$\dot{\gamma}_{\text{eff}}$ = Effective particle shear rate

$\dot{\gamma}_{NL}$ = Nonlocal shear rate

$\boldsymbol{Q}$ = Anisotropy stress tensor

(Morris & Boulay, *J. Rheol.*, 1999; Zarraga *et al.*, *J. Rheol.*, 2000; Dbouk *et al.*, *J. Non-Newtonian Fluid Mech.*, 2003)

A novel thermo-rheological migration force

- To rationalize thermal-shear effect, consider forces acting on particle phase:
- Compute force on particle phase as $\boldsymbol{f}_\Sigma = \nabla \cdot \boldsymbol{\Sigma}_p$
- So, $\boldsymbol{f}_\Sigma = \nabla \cdot (2\mu_p \dot{\boldsymbol{S}}_p - \mu_f \eta_N(\phi)\dot{\gamma}_{\text{eff}} \boldsymbol{Q})$
- For 1D flow this looks like

$$f_\Sigma = \underbrace{A(\phi)\mu_f \left(\frac{d\dot{\gamma}}{dx}\right)}_{\text{shear-induced particle migration flux}} \underbrace{- A(\phi)\dot{\gamma}_{\text{eff}} \left|\frac{d\mu_f}{dT_f}\right| \left(\frac{dT_f}{dx}\right)}_{\text{new thermo-rheological flux}} + \underbrace{\mu_f \dot{\gamma}_{\text{eff}} \left(\frac{dA(\phi)}{d\phi}\right)\left(\frac{d\phi}{dx}\right)}_{\text{effect of particle concentration ~ negligible}}$$

flux due to shear gradient **opposes** thermo-rheological flux!

Let $A(\phi) = -\sqrt{2}\eta - \eta_N$

(Nagrani, Municchi, Marconnet & Christov, *Int. J. Heat Mass Transf.,* 2022)

Model calibration

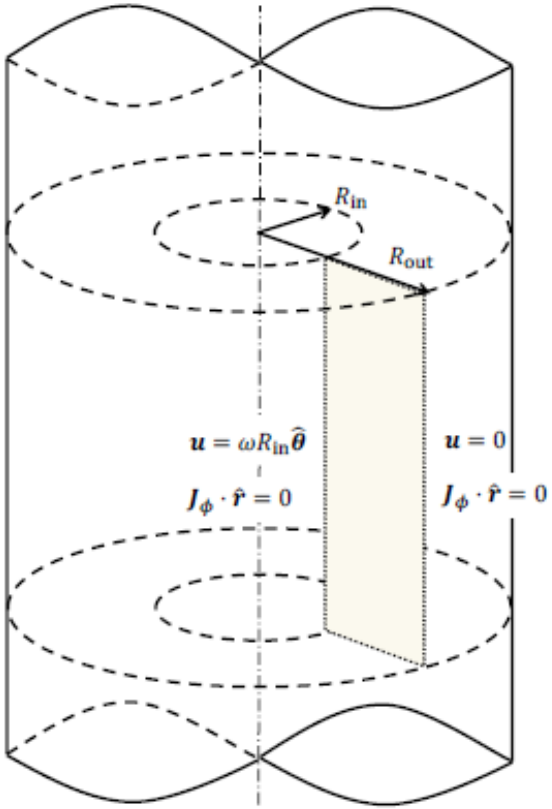

(Municchi, Nagrani & Christov, *Int. J. Multiphase Flow*, 2019)

Boundary conditions		on inner wall	on outer wall
$t < 5$ s	Velocity	$\boldsymbol{u} = \boldsymbol{0}$	$\boldsymbol{u} = \boldsymbol{0}$
	Temperature	$T = 298K$	$\nabla T \cdot \hat{\boldsymbol{n}} = 0$
$t > 5$ s	Velocity	$\boldsymbol{u} = \omega R_{in}\hat{\boldsymbol{\theta}}$	$\boldsymbol{u} = \boldsymbol{0}$
	Temperature	$\nabla T \cdot \hat{\boldsymbol{n}} = 0$	$\nabla T \cdot \hat{\boldsymbol{n}} = 0$

initial temperature = 293 K

Temperature decay curve:

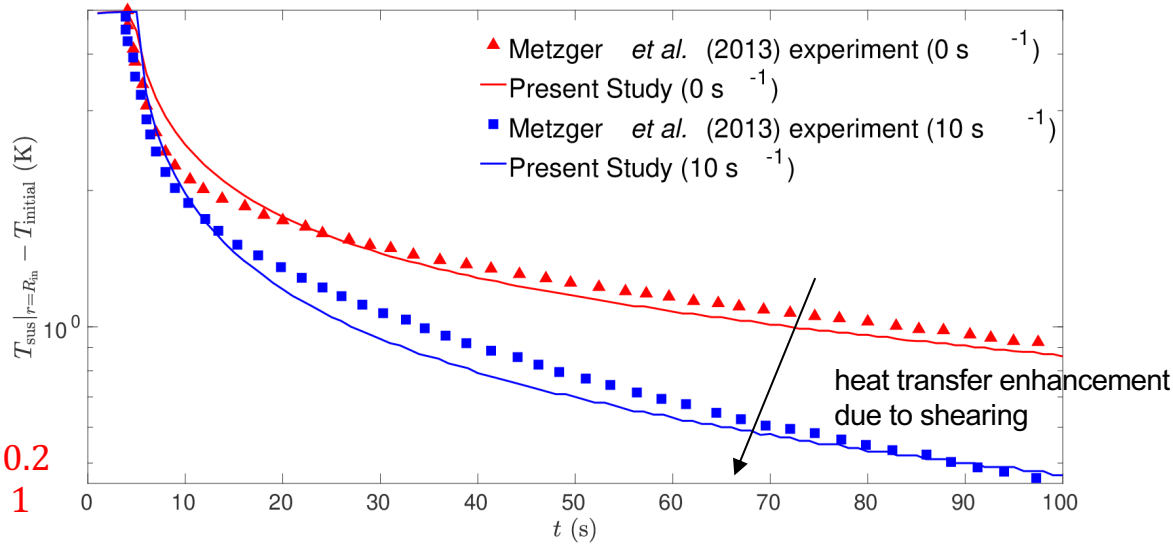

$$\Rightarrow K_h = K_{h_o}\left(1 + \beta\phi\left(\frac{||\dot{\boldsymbol{S}}_{\boldsymbol{p}}||d_p^2}{\alpha_p}\right)^m\right)$$

$\beta = 0.2$
$m = 1$

Thermal vs. shear gradients in the Couette cell

Computational domain and setup

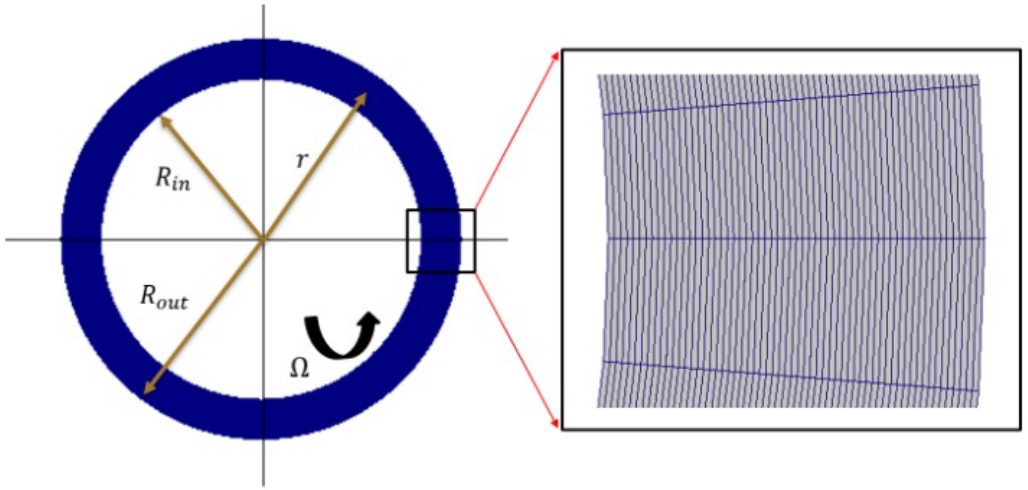

Thermal BCs	T_{in}	T_{out}
Case 1: Migration with thermal gradient	323 K	293 K
Case 2: Migration against thermal gradient	293 K	323 K

Aim: vary the direction of thermo-rheological flux.

- Axisymmetric – 1D simulation
- Orthogonal structured mesh
- Transient formulation – 2000 seconds

3M Fluroinert Electronic Liquid FC43 Datasheet (Sept. 2019)

Properties	Thermal conductivity $\left(\frac{W}{m\,K}\right)$	Density $\left(\frac{kg}{m^3}\right)$	Specific heat $\left(\frac{J}{kg\,K}\right)$	Viscosity $(Pa \cdot s)$
Particles	35.5	1900	960	–
Fluid	0.05601 – 0.0656	1570.4 – 1900	1045.08 – 1257.97	0.0012 – 0.0047

Suspension of Boron Nitride (BN) particles & Fluorinert (FC-43) fluid

Thermal boundary conditions control particle migration

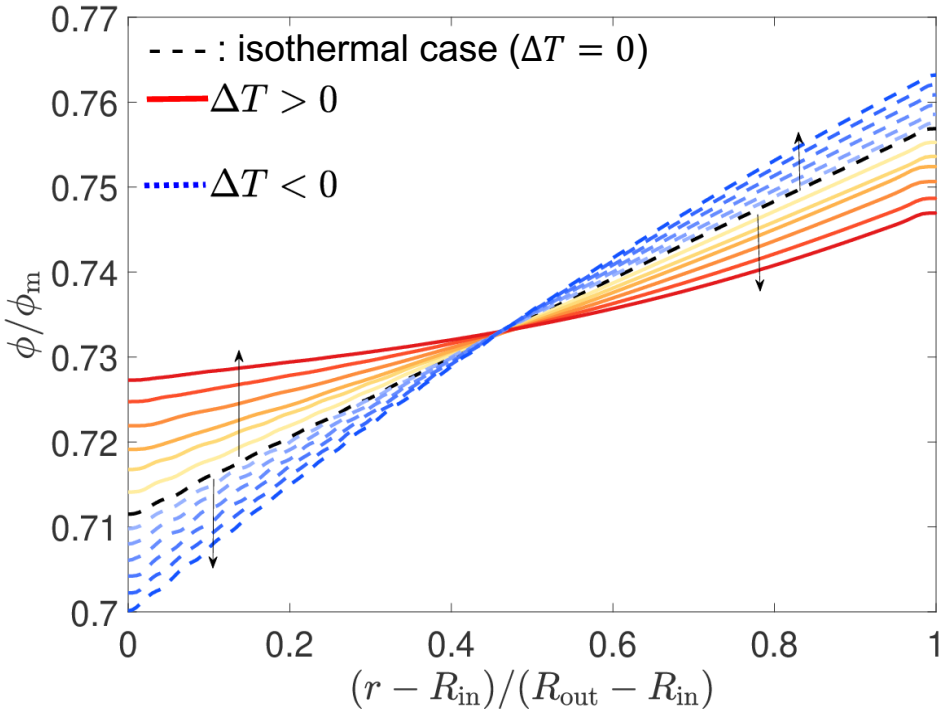

- $\Delta T > 0$: Flux due shear gradients **opposed** by flux due to thermal gradients.
- $\Delta T < 0$: Flux due to shear gradients **aided** by flux due to thermal gradients.
  - As $|\Delta T|$ increases, the thermo-rheological flux enhances migration.

(Guazzelli & Morris, 2011)

- Starting from homogenous initial particle distribution at $t = 0$.

(Nagrani, Municchi, Marconnet & Christov, *Int. J. Heat Mass Transf.*, 2022)

Strongly sheared suspensions are more homogeneous

$\boldsymbol{Pe}_{\mathrm{th}}$ controls the interplay between thermal and shear particle migration

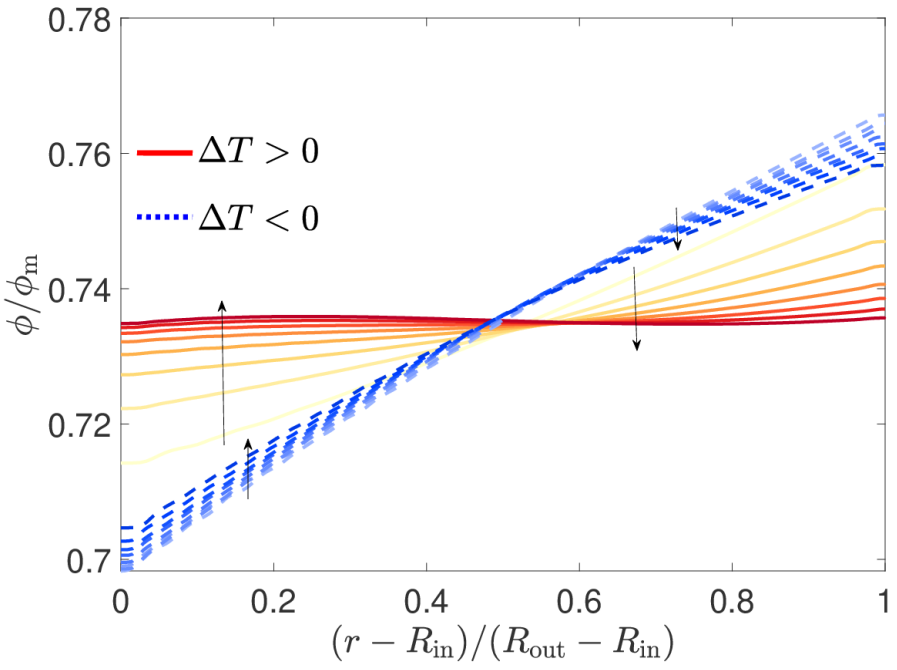

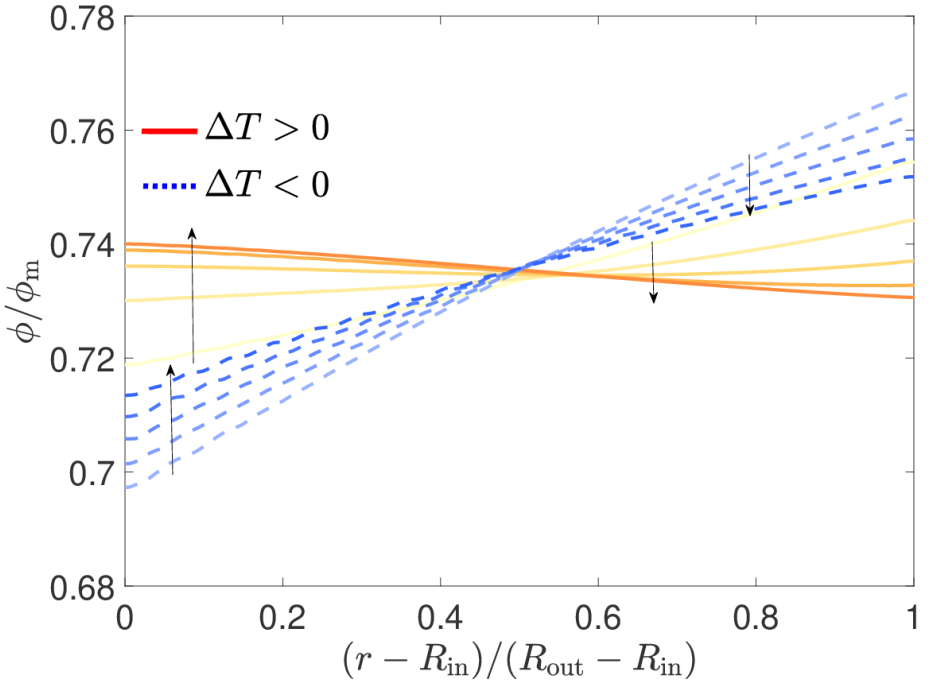

- For both thermal BCs, particle migration suppressed for larger $Pe_{\mathrm{th}} = \frac{\dot{\gamma} d_p^2}{\alpha_p}$.
- $\Delta T > 0$: **opposing** thermal and shear fluxes ⇒ more homogenous particle distribution.
- $\Delta T < 0$: **augmenting** thermal and shear fluxes ⇒ significant particle migration.

Electronics cooling via dense suspensions

Microchannel geometries

(All dimensions in mm)

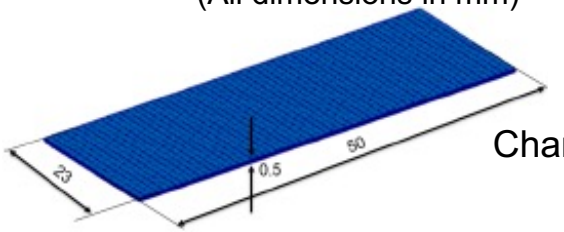

(a) Uniform cross-section channel.

Channel Height: 0.5mm

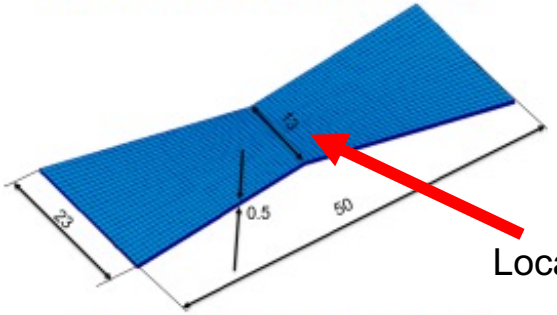

(b) Converging-diverging channel.

Local *Re* enhancement

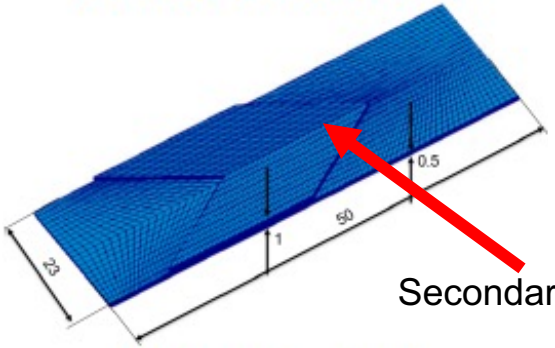

(c) Herringbone channel.

Secondary flows: eddies

Boundary conditions and simulation setup

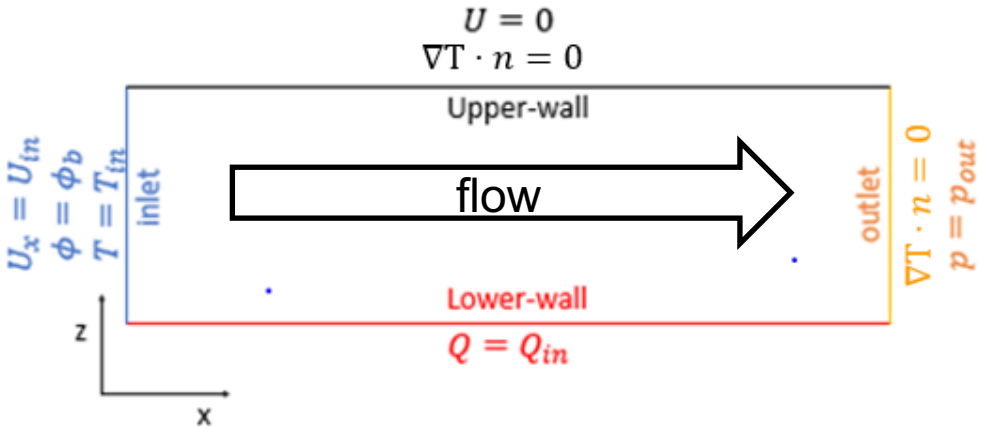

- Suspension comprised of $50\ \mu m$ Boron Nitride particles at 30% concentration in an FC-43 fluid.
- Time to steady state ≈ 300 seconds.

Hot-spot cooled with FC-43 fluid

Consider cooling a 2 W/cm^2 hot spot using a dielectric fluid (FC-43):

Straight channel

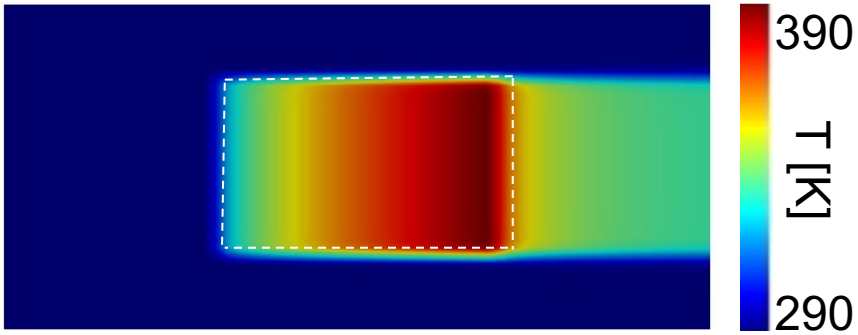

Poor thermal spreading leads to high temperature rise

Changing the channel geometry can modify performance:

Herringbone channel

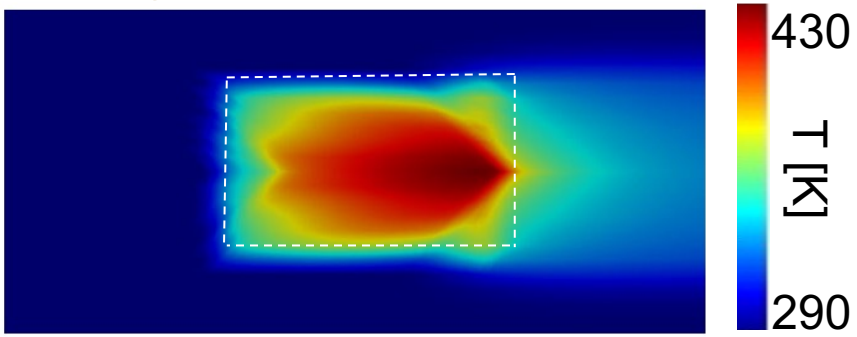

converging--diverging channel

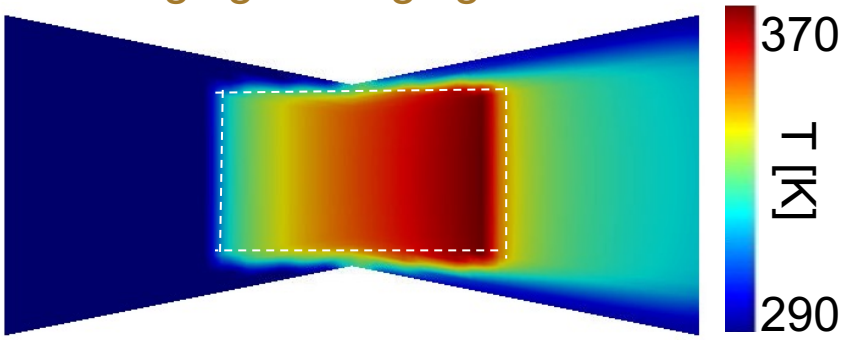

Dense suspensions can reduce junction temperatures by enhancing spreading

Dielectric Fluid (FC-Fluid) + **High Thermal Conductivity Particles (Boron-Nitride)**

Hot-spot cooled with suspension

Consider cooling a 2 W/cm^2 hot spot using suspensions:

straight channel

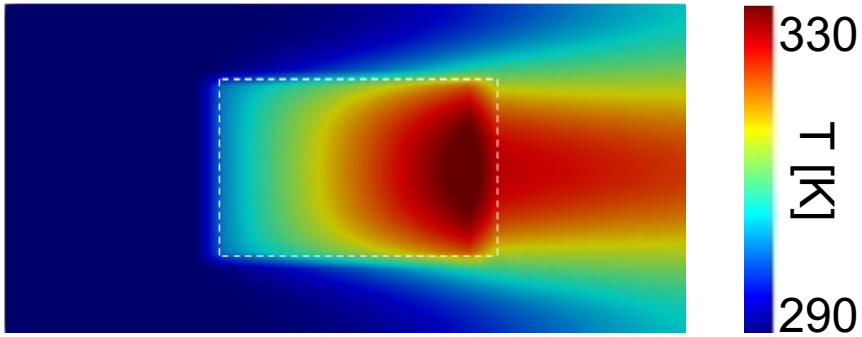

High conductivity suspensions enhance thermal spreading, improving performance

Changing the channel geometry can modify performance:

herringbone channel

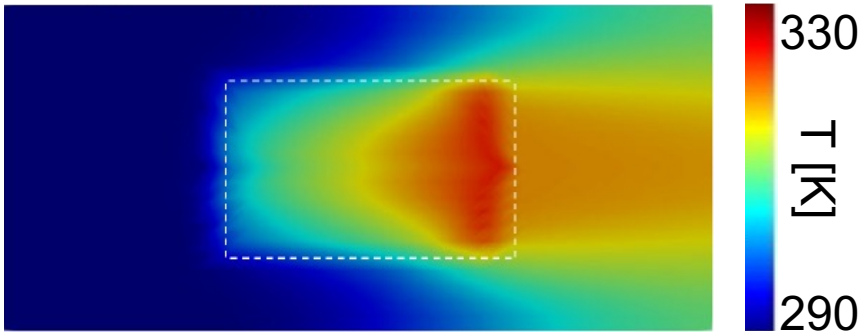

converging--diverging channel

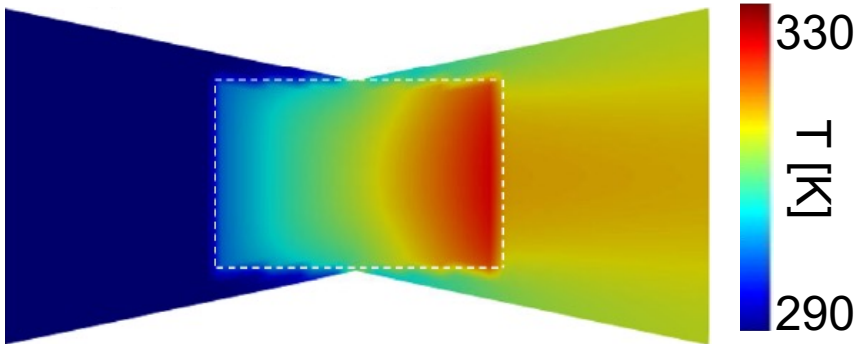

Dense suspensions reduce junction temperatures by 100 K

(Nagrani, Christov, and Marconnet, IEEE-ITherm:, 2021)

Hot-spot cooling: FC-43 vs. suspension

FC-43 fluid

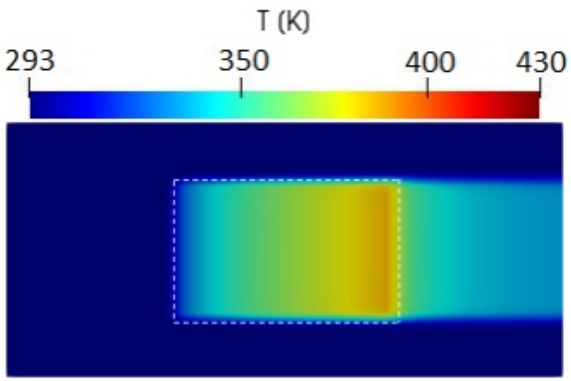

(a) Uniform cross-section channel.

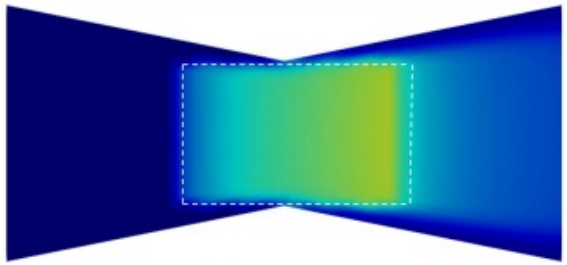

(b) Converging-diverging channel.

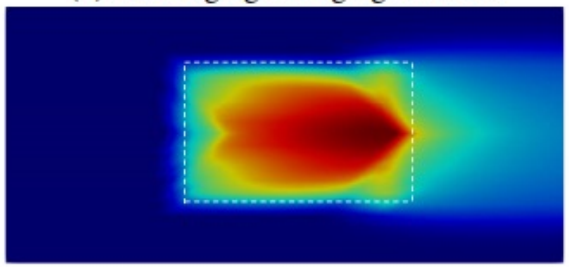

(c) Herringbone channel.

suspension

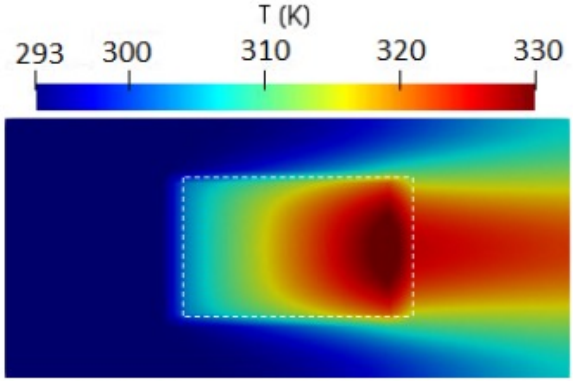

(a) Uniform cross-section channel.

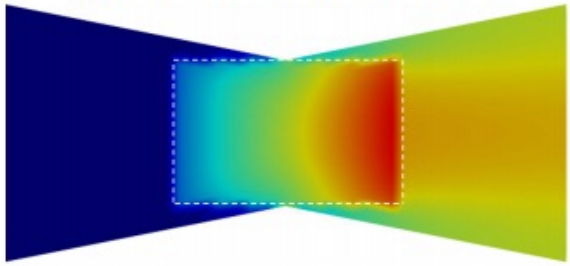

(b) Converging-diverging channel.

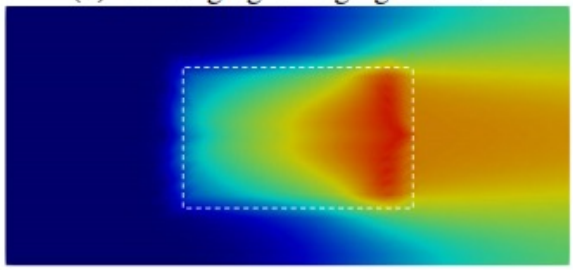

(c) Herringbone channel.

- Negligible thermal spreading with pure FC-43 fluid.
- Appreciable thermal spreading with suspension.
  - Better thermal management!

(Nagrani, Christov, and Marconnet, IEEE-ITherm:, 2021)

Hot-spot cooling: local HTC

Axial variation of the heat transfer coefficient (HTC)

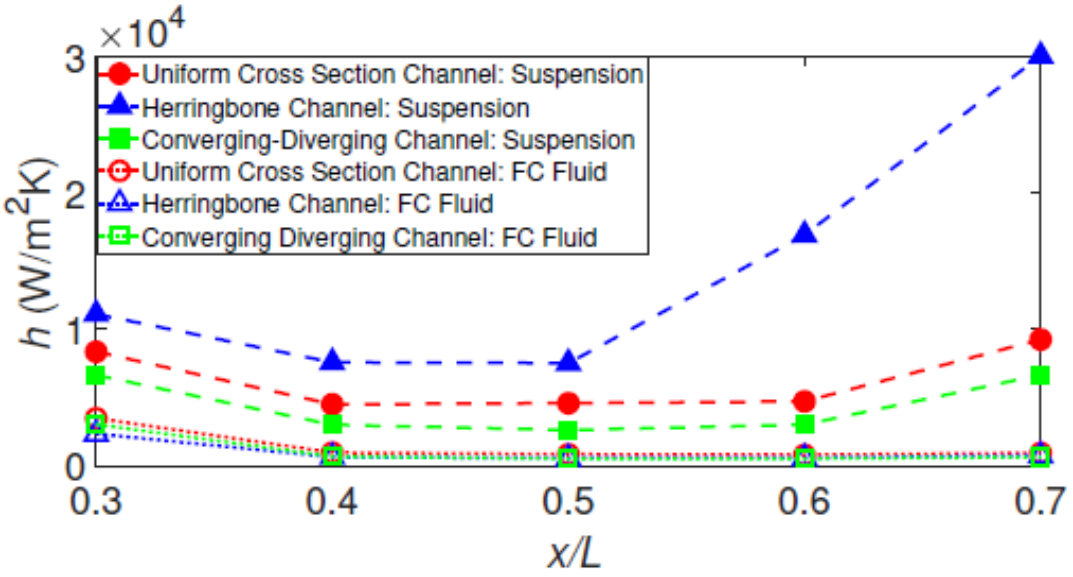

- Trend for pure FC-43 fluid follows analytical expressions from textbooks.
- HTC for suspensions is higher.
- **Sharp rise in the case of herringbone channel due to secondary flow in notch.**

Particle concentration distribution $\phi(x,t)$ in a herringbone channel

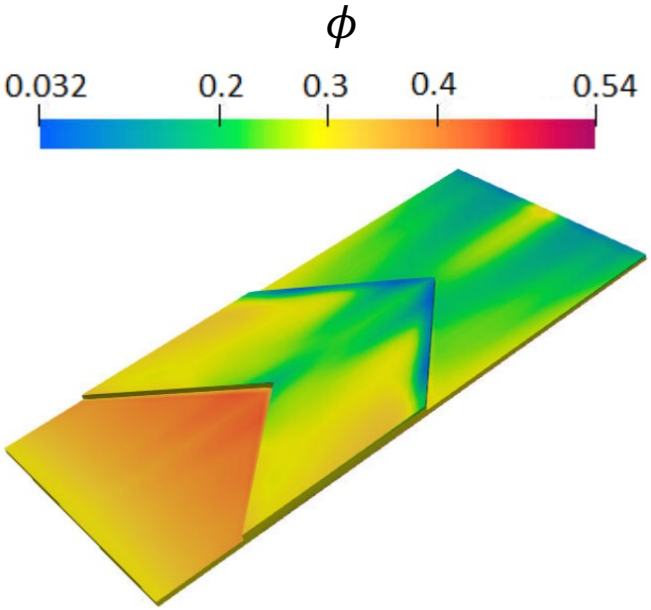

(Nagrani, Christov, and Marconnet, IEEE-ITherm:, 2021)

Constant heat flux of 5W: FC-43 vs. suspension

FC-43 fluid

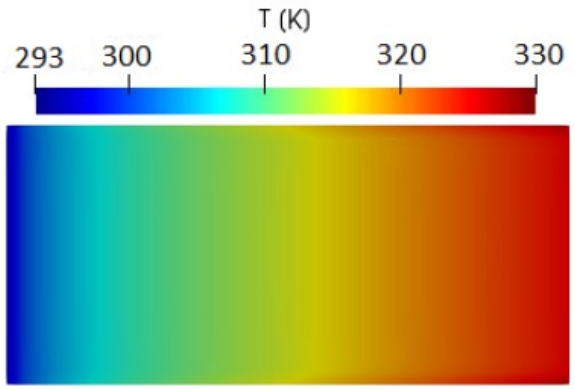

(a) Uniform cross-section channel.

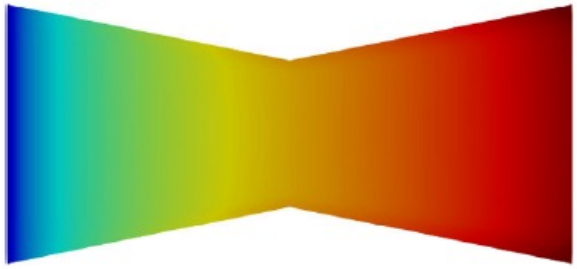

(b) Converging-diverging channel.

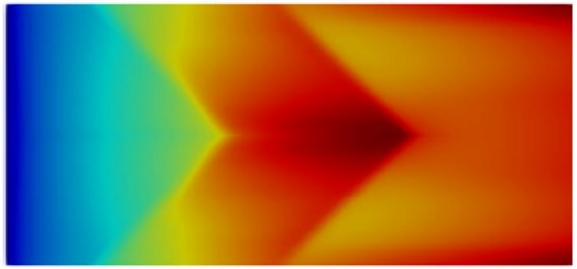

(c) Herringbone channel.

suspension

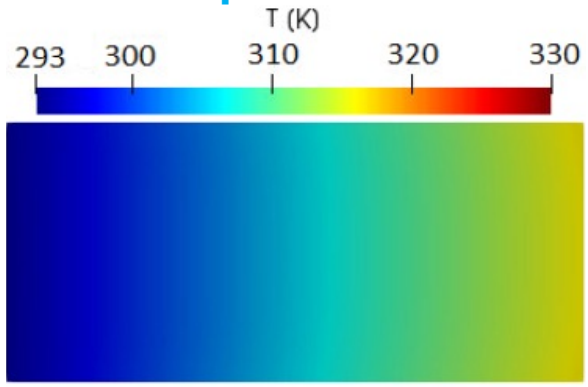

(a) Uniform cross-section channel.

(b) Converging-diverging channel.

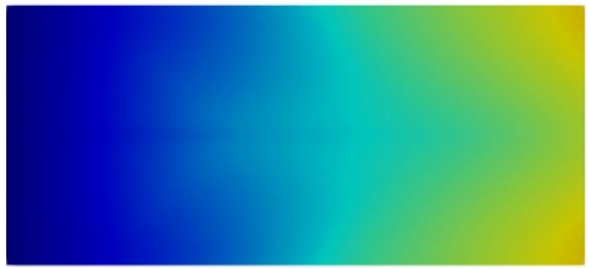

(c) Herringbone channel.

- Uniform base heating: suspension reduced max. temp. rise by 15 K.
- Similar max. temp. in all three microchannels with a suspension.
- Impact of thermal spreading reduced due to uniform heating of the base.

Nagrani, Christov, and Marconnet, IEEE-ITherm:, 2021

Constant heat flux:
Local heat transfer coefficient & pumping power

Axial variaton of heat transfer coefficient

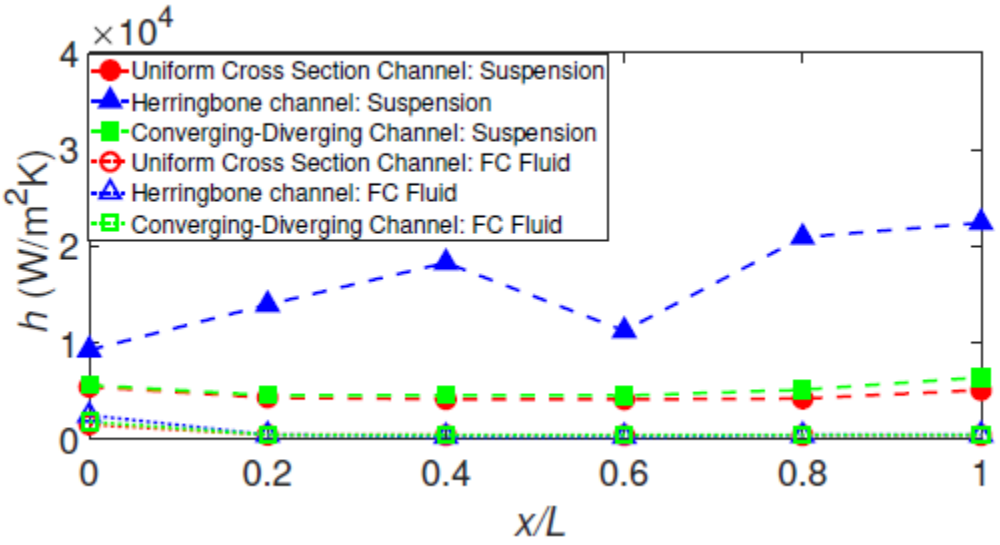

- Higher heat transfer coefficient in suspensions owing to better properties.
- Highest thermal transport rate in herringbone channel.

Pumping power

- High pumping power for suspension:
  - highest pumping power in converging-diverging channel.

Microchannel Geometry	Pumping Power (μW)			
	FC-43 Fluid		Suspension	
	Uniform	HS	Uniform	HS
Uniform cross-section channel	9.1	9.2	19.8	21.3
Converging-diverging channel	11.6	12.5	27.1	26.7
Herringbone channel	5.7	5.8	8.5	8.6

Conclusion

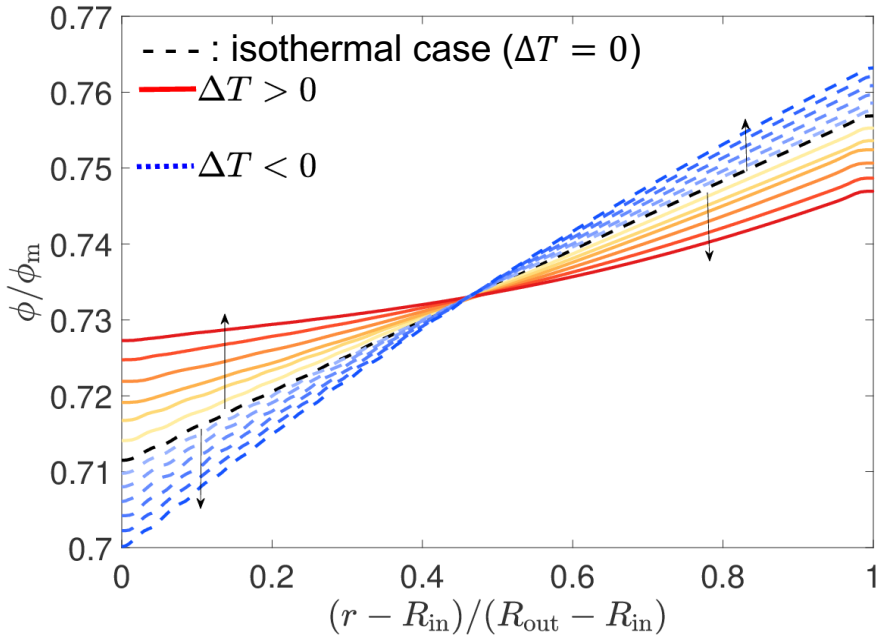

- Particle migration can be **enhanced or suppressed** depending upon the direction of heat transfer.

(Nagrani, Municchi, Marconnet & Christov, *Int. J. Heat Mass Transf.,* 2022)

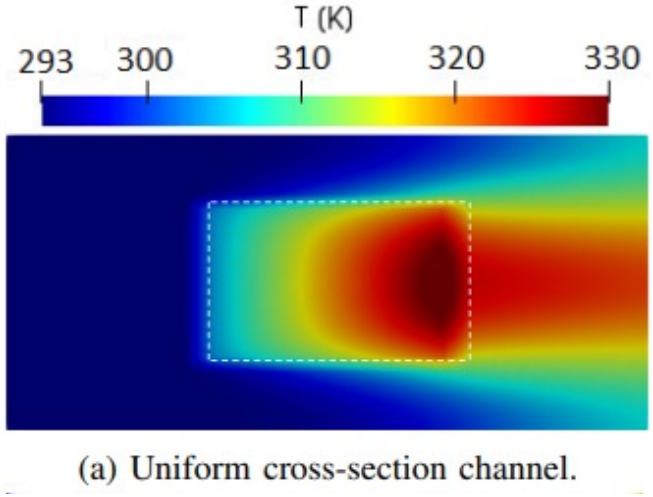

(a) Uniform cross-section channel.

- Suspensions **reduce junction-level temp. for hot-spot** heating due to enhanced thermal spreading via particle migration.

(Nagrani, Christov, and Marconnet, IEEE-ITherm:, 2021)

Thank you for your attention!
Questions?

- Further reading:
  - P.P. Nagrani, F. Municchi, A.M. Marconnet, I.C. Christov, "Two fluid modeling of heat transfer in flows of dense suspensions," *Int. J. Heat Mass Transf.,* 2022, **arXiv: 2105.08853**.
  - F. Municchi, P.P. Nagrani, I.C. Christov, "A two-fluid model for numerical simulation of shear-dominated suspension flows," *Int. J. Multiphase Flow,* 2019, **arXiv:1811.06972**.